

Effect of Bimetal Oxide ZnO/ZnS Nanocomposite Doped TiO₂ on the Performance of Dye-Sensitized Solar Cell

Hind Jameel Owaid¹, Taghreed Baqer Alwan¹, Saifaldeen Muwafaq Abdalhadi^{2,*}

¹Department of Chemistry, Ibn Al-Haitham College of Education for Pure Science, Baghdad University, Baghdad, Baghdad, Iraq

²Remote Sensing Department, College of Remote Sensing and Geophysics, Al-Karkh University of Science, Baghdad, Iraq

Article's Information

Received: 23.06.2024
Accepted: 29.07.2024
Published: 15.03.2025

Keywords:

Dye-sensitized solar cells,
photoanode,
TiO₂,
metal oxide,
nanocomposite

Abstract

Dye-sensitized solar cells (DSSC) have garnered significant interest in recent years because of their comparatively affordable production expenses and the potential to utilize flexible and transparent substrates. A widely used approach to enhance the efficiency of DSSCs is the optimization of the photoanode components by the introduction of metal or metal oxide doping in TiO₂ nanostructures. In this work, the exclusive gel technique is used to produce nanoparticles of TiO₂, ZnO, and ZnS. Additionally, we prepared a ZnO/ZnS nanocomposite by mixing these materials in specific weights in an ethanolic solution. All prepared materials were characterized using scanning electron microscopy (SEM), energy-dispersive X-ray spectroscopy (EDX), and high-resolution X-ray diffraction (XRD). The doctor blade approach was used to prepare three kinds of photoanode in DSSC. These photoanodes were made by adding a co-dopant, ZnO/ZnS, in different weights (2%, 4%, and 6%) into TiO₂ nanoparticles. The 6% wt of ZnO/ZnS doped TiO₂ resulted in an enhancement in power conversion efficiency (PCE), reaching 4.92 %. This may be attributed to an increase in the short-circuit current density (J_{sc}) to 9.60 mA/cm² and the open-circuit voltage (V_{oc}) to 0.81 V, which represents a 20% enhancement compared to the undoped photoanode.

<http://doi.org/10.22401/ANJS.28.1.04>

*Corresponding author: dr.saifaldeen@kus.edu.iq



This work is licensed under a [Creative Commons Attribution 4.0 International License](https://creativecommons.org/licenses/by/4.0/)

1. Introduction

Energy is one of the most important requirements for development as well as a key source of economic growth. Many promising technologies are being reported in the direction of harnessing energy from renewable sources [1]. Solar cells are important and have become quite popular for their worldwide applications [2]. However, the commercial success of any solar-cell technology depends on the manufactured cost per unit watt. The cost is very high for the preparation and purification of commercial solar cells, such as monocrystalline Si, polycrystalline Si, and amorphous Si, [3, 4], which leads to an increase in the cost of the individual solar-cell units. Therefore, Dye-sensitized solar cell (DSSC) is a third-generation photovoltaic (PV) technology

that is an alternative to the conventional types of solar cells [5, 6]. The main advantages of the DSSC represent the best utilization of incident photons and the possibility of fabricating large-area, lightweight, flexible, and lower-cost ultrathin devices using a fast, low-temperature fabrication process [7,8]. The structure of a typical DSSC consists of a number of components such as transparent conducting oxide (TCO) coated glass slide that serves as the conducting and collecting electrode, a layer of highly porous metal oxide coated on TCO slide for the electron transportation, a sensitizer such as organic or organometallic dye adsorbed in the metal oxide layer for the light-absorption, a layer of solid electrolyte covering the metal oxide layer, a counter electrode opposing to the nanoparticle layer to complete the

circuit and a thin polymer spacer separating the two electrodes to prevent a short contact. The high dyed absorption, efficient charging across the nanoporous metal oxide layer, and catalytic electrode reaction of each component are vital to achieving high photoconversion efficiency. The electrical energy is actually generated by the flow of photogenerated electrons via an external load. The efficiency and stability of each component determine the performance and reliability of the DSSC [9-12]. In DSSCs, mesoporous semiconductor photoanodes are crucial in light adsorption, electron transport and collection [13]. However, the development of an effective nanomaterial photoanode is very important for DSSCs in converting sunlight into photo-excited electrons [14]. Titanium dioxide (TiO₂) has been paid special attention due to its high charge separation efficiency, both electron and hole mobility network, large surface area, and the advantage of easy fabrication of large-area and thin films [15-17]. Especially the high chemical stability and the capability of inserting various metal complexes, noble metals, or other oxides in nanoporous TiO₂ thin film make it the most employed photoanode for DSSCs. Additionally, inorganic semiconductors such as ZnS [18], CdS [19], SnO₂ [20], and WO₃ [21] have been studied as the photoanodes of DSSC. Out of the various inorganic materials, ZnS has gained much attention both from experimental and theoretical perspectives. ZnS is a wide band gap (3.7 eV), n-type direct semiconductor with a large exciton energy (26-60 mV), which has opened up a whole new area for creating nanoscale devices such as blue- and green-emitting electroluminescent diodes, field-emission displays, photoconductors, and solar cells [22-24]. Varieties of metal oxide nanoparticles such as ZnO [25], Fe₃O₄ [26], and Fe₂O₃ [27] are also used as photoanodes, and each showed a significant effect on photon-to-electron conversion efficiency based on their sizes and surface areas. In this paper, we prepared bimetal oxide ZnO/ZnS and co-doped it in a different ratio (2%, 4%, and 6%) in TiO₂ to improve the performance of the photoanode in DSSC.

1. Materials and Methods.

1.1. General information

All starting materials and solvents were supplied by TCI and Alfa Aesar, and all chemicals were used without any purification. The structures, components of the materials, and morphologies of all prepared nanoparticles were recorded using a scanning electron microscope (SEM) and energy-dispersive X-ray spectroscopy (EDS) JOEL JSM-6460LV. The high-resolution X-ray diffraction XRD was obtained by Lab X- XRD 6000, Shimadzu, Japan

1.2. Synthesis method

- a. **Synthesis of TiO₂ nanoparticles:** Synthesis of TiO₂ NPs were described in previous work [28], with some modifications. 10 mL of Ti(OBu)₄ was dissolved in 10 mL of absolute ethanol, and the mixture was left to stir for 15 min. Meanwhile, 2 mL of (65%) HNO₃ and 10 mL of deionized water were added to another 40 mL of absolute ethanol, then the mixture of Ti(OBu)₄ was added dropwise to the acidic mixture and stirred for 20 min at room temperature. The clear transparent sol-gel appeared after 2 h; the obtained residue was then separated by centrifuge. The solid residue was dried at 75 °C for 10 h in air and then calcined at 400 °C for 3 h.
- b. **Synthesis of ZnO nanoparticles:** Synthesis of ZnO NPs were described in previous work [29]. 4.16 g of Zn(Ac)₂·2H₂O was dissolved in 100 mL deionized water and stirred for 15 min. 3.5 g of NaOH was dissolved in 100 mL of deionized water and then dropped above the prepared zinc acetate solution. The mixture was left to stir for 1 h until the precipitate appeared. The precipitate was separated and collected by centrifuge, then washed several times with deionized water. The prepared ZnO nanoparticles were heated at 70 °C for 10 h in an air and then calcined at 400 °C for 3 h.
- c. **Synthesis of ZnS nanoparticles:** Synthesis of ZnS NPs were described in previous work [30]. The co-precipitation technique was used to prepare ZnS nanoparticles. 3.87 g of Na₂S·9H₂O was dissolved in 100 ml of distilled water with a stir in the solution for 15 min. Then 2.83 g of ZnCl₂ was dissolved in 100 ml of distilled water with a stir at room temperature for 15 min. The two prepared solutions were mixed with each other, and then a few drops of NaOH were added with a stir for 30 min; after that, the white color precipitate appeared due to the formation of ZnS. The precipitate was washed several times in distilled water. The prepared ZnO nanoparticles were heated at 70 C for 10 h in an air and then calcined at 400 C for 3 h
- d. **Synthesis of ZnO/ZnS nanocomposite,** 0.01mole of ZnO NPs was mixed with 0.01 mole of ZnS NPs in 50 mL of acetone. The mixture was vigorously stirred for 30 min, dried under vacuum, and heated at 100 °C in an oven [24].

1.3. Modification of DSSCs

DSSCs were modified by different working electrodes using a ZnO/ZnS as a co-doped in different weight (2 wt%, 4 wt%, and 6 wt%) in mesoporous TiO₂ NPs film, as shown in Figure 1. Photoanodes were made by grinding the TiO₂ powder into a mortar and pestle to improve its homogeneity. A paste was then made by adding ethylene glycol to the powder at a 1:2 ratio and grinding for 5 minutes. A different quantity of ZnO/ZnS (2 wt%, 4 wt%, and 6 wt%) was added to this paste and mixed until homogeneity was improved. The paste was then coated onto an indium tin oxide (ITO) glass sheet using the doctor blade

method [6] with a thickness of approximately 4 mm. The coated substrate was then sintered in a hotplate at 250 °C for half an hour. After the ZnO/ZnS co-doped TiO₂ layer was cooled, the electrode was immersed in a diluted solution of dye N912 (1 × 10⁻³ M) for about 24 h to allow adsorption of the dye molecules onto the TiO₂ surface. The Au counter electrode of the DSSCs was prepared by thermal evaporating. The working electrode was clamped with the counter electrode after adding redox electrolyte solution (I^{3-/3I⁻}). Finally, the prepared DSSCs were tested in photovoltaics measurement devices.

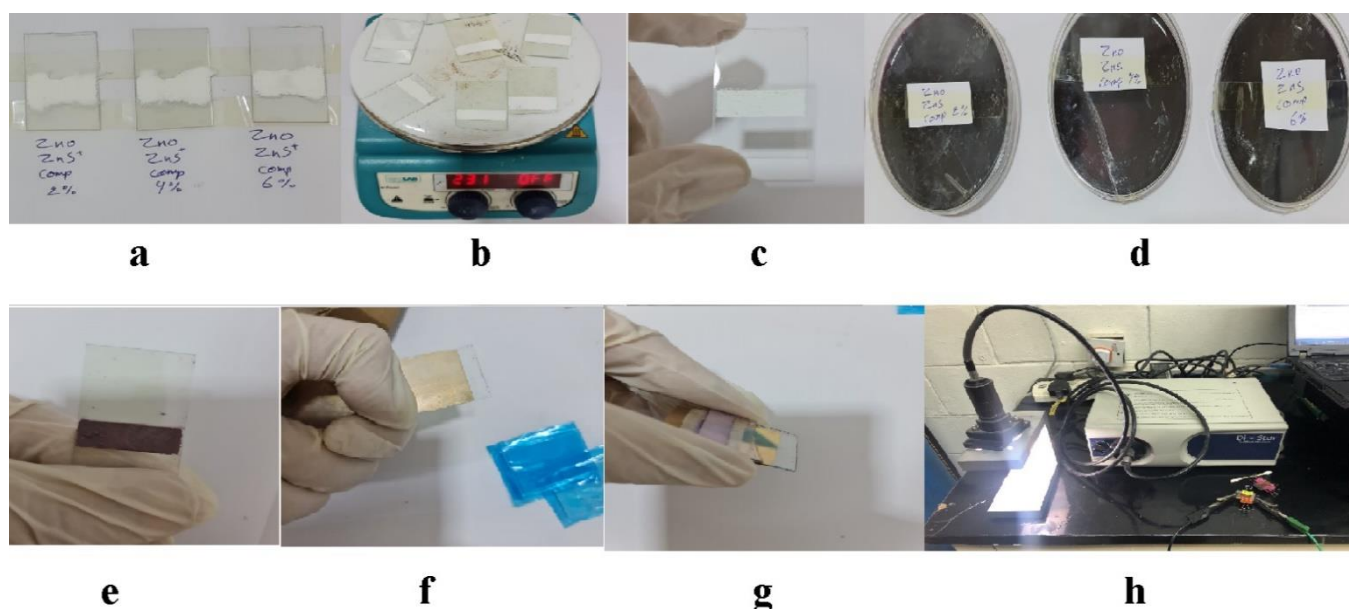


Figure 1. Modification of DSSCs: a. paste coated in ITO glass sheet, b. aneling of paste at 250 °C. c., d., and e. the photoanode coated in dye (N790), f. gold counter electrode, g. modified DSSC and h. DSSCs tested.

2. Results and Discussion

2.1. Nanoparticals characterization

Figure 2 illustrates the XRD of all prepared compounds. All the peaks are intense and sharp, which indicates that all the synthesized materials have an excellent crystalline phase. TiO₂ pattern (Figure (2a)) shows a tetragonal anatase phase with a clear diffraction form at the (101), (004), (200), (105), (211), (204), (110), (220), and (215), which agreement with standard data (JCPDS card no. 21-1272). The XRD pattern of ZnO (Figure. 2(b)) illustrates the hexagonal wurtzite phase with

corresponding Miller indices (hkl) of (100), (002), (101), (102), (110), (103), (200), (112), and (201) respectively, and that was an agreement with standard data (JCPDS card no. 00-036-1451) [24]. The pure cubic phase of ZnS was presented in an XRD pattern (Figure (2c)) with a clear diffraction form at the (111), (220), and (311), and that was in agreement with the standard data (JCPDS card No.80-0020). The XRD of mixing nanocomposite ZnO/ZnS illustrates all diffraction peaks for ZnO (hexagonal wurtzite phase) and ZnS (cubic phase).

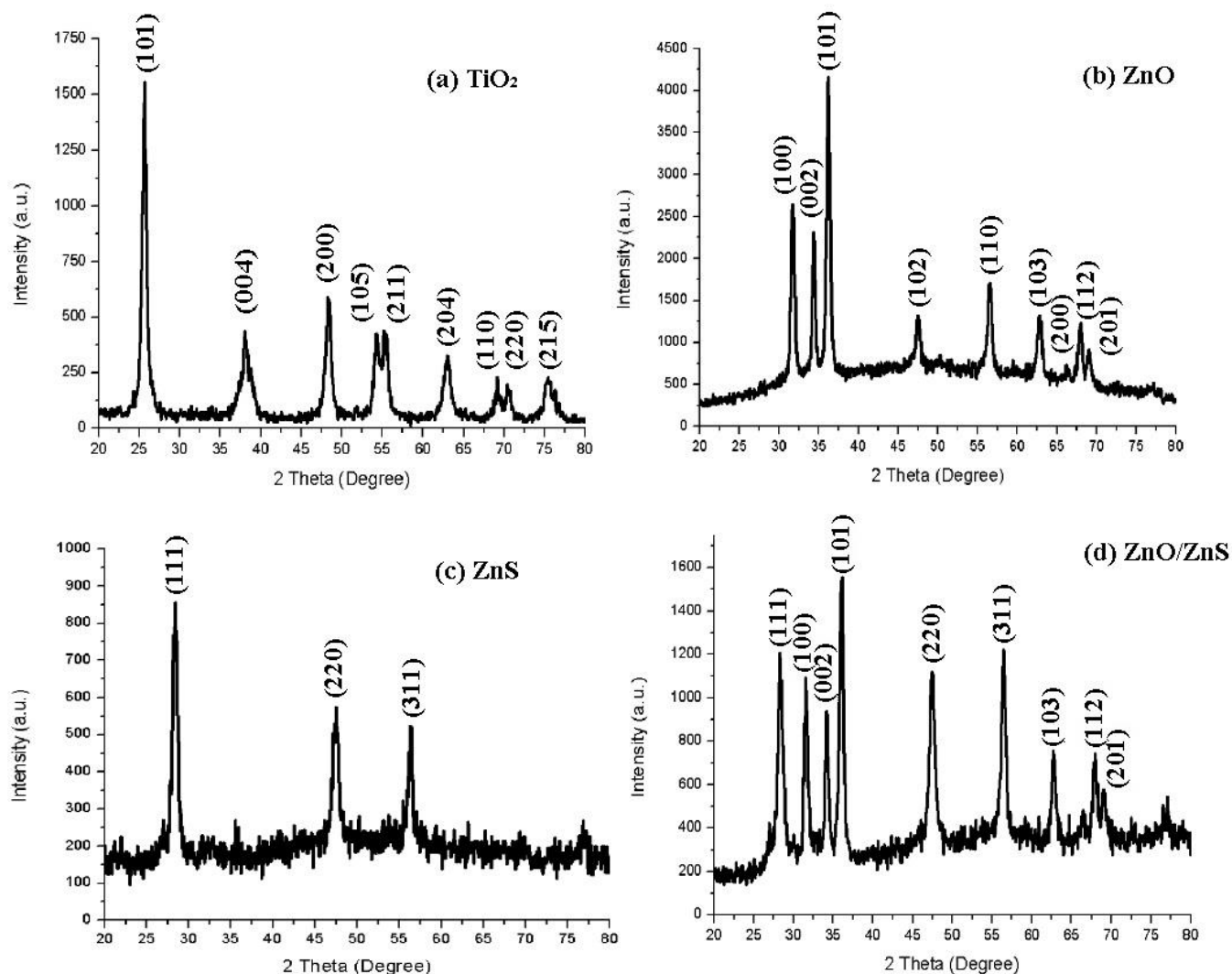


Figure 2. XRD pattern of a) TiO_2 , b) ZnO , c) ZnS , d) ZnO/ZnS

An SEM study was conducted to examine the morphology of the thin film and determine its homogeneity, crystallite size, and the presence of any secondary phases in the ZnO/ZnS nanocomposite. Figure 3 displays scanning electron microscope (SEM) images of pure TiO_2 , ZnO , ZnS , and a ZnO/ZnS composite at various magnifications. The scanning electron microscope (SEM) picture of TiO_2 reveals that the film has a granular and rough texture. This characteristic makes it an ideal material for the photoanode of a dye-sensitized solar cell (DSSC). The roughness of the film indicates that it has a high capacity to scatter light, which in turn enhances its potential to collect light effectively from the cell. While the film's porosity nature is beneficial for facilitating the diffusion and adherence of dye to the

film, it poses a significant drawback for charge transmission owing to the resistive hopping mode between particles. The TiO_2 has a grain size of around 12 nm. The higher magnification picture reveals that the ZnS grains have a somewhat consistent and homogeneous structure, with an average dimension of roughly 30 nm. The ZnO/ZnS nanocomposite exhibits distinct features when seen at various levels of magnification. The photos clearly show that the two metal oxides are well blended, with no indication of any metal oxide forming on top of the other. This conclusion is significant because if one oxide is placed on top of the other, it will lead to the trapping of charges at the dye/sensitizer, which would prevent the injection of electrons into the conductive substrate.

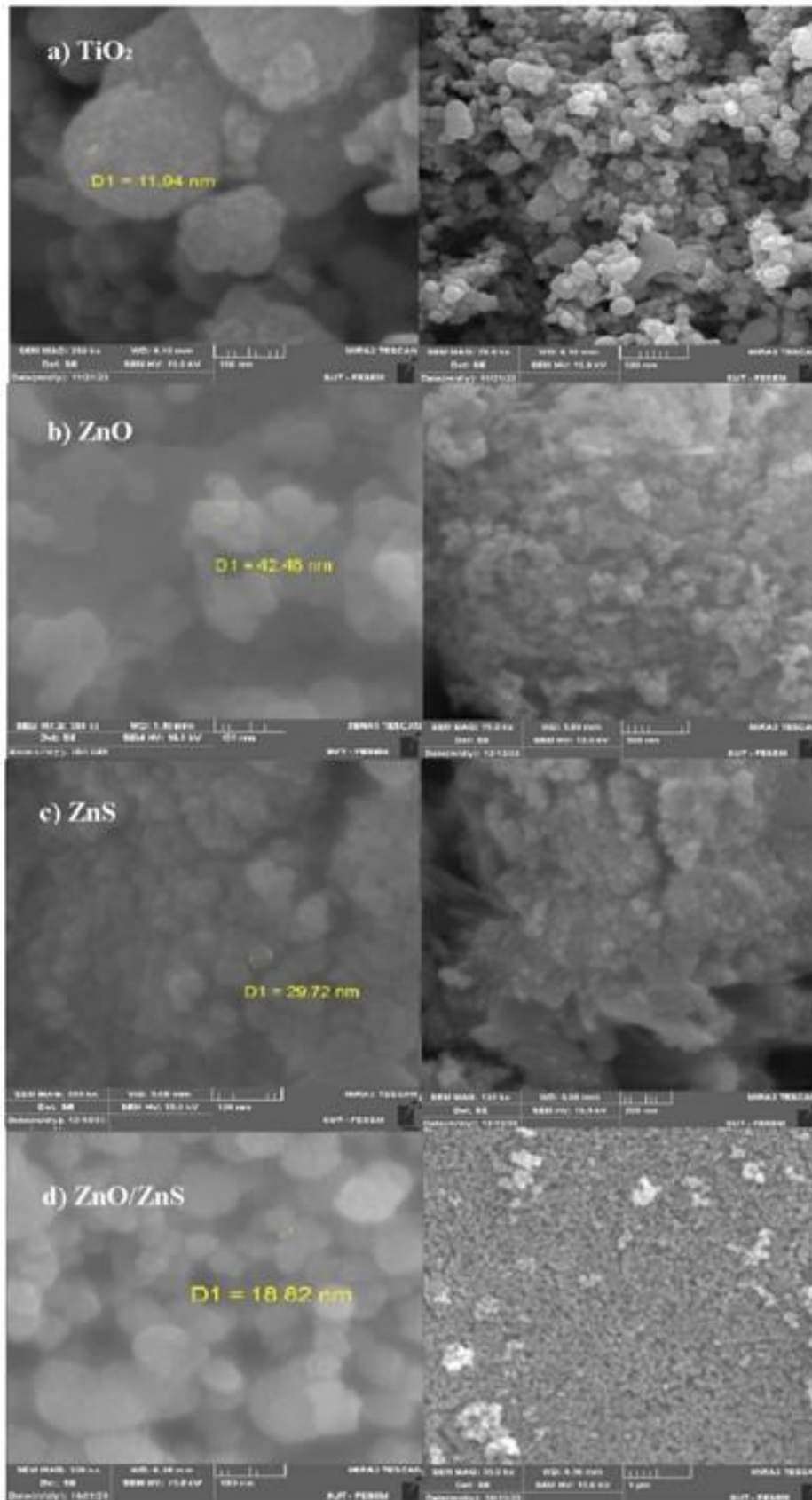


Figure 3. SEM images of preparing nanoparticles a) TiO₂, b) ZnO, c) ZnS, d) ZnO/ZnS

An EDX test was conducted to determine the elemental composition and chemical analysis of the produced nanoparticles. Figure 4 displays the outcome of the EDX study. Overall, it was determined that all of the samples contained just the original constituents, and no additional elements were discovered. Furthermore, it is noteworthy to demonstrate that the atomic percentages of 100%

indicate that the observed amounts of Zn, S, and O in the nanocomposite are almost in a stoichiometric ratio. The absence of data measurement from the precipitated impurities may be attributed to the fact that the EDX measurement region was limited to the ZnO and ZnS crystals. The EDX-mapping analysis has shown that the ZnO/ZnS sample exhibits a high degree of uniformity [18].

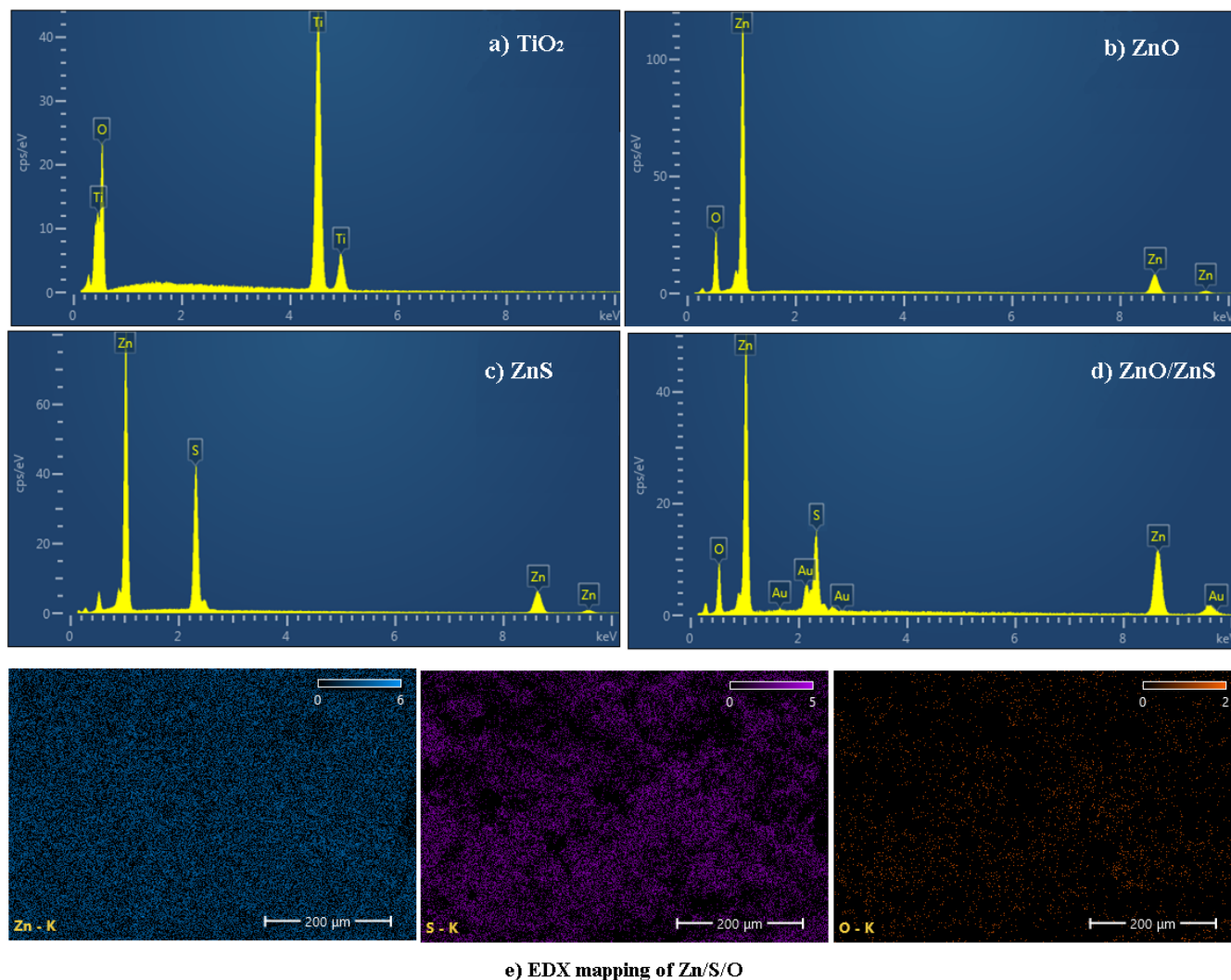


Figure 4. EDX analysis of a) TiO₂, b) ZnO, c) ZnS, d) ZnO/ZnS e) mapping of Zn/S/O

2.2. Device Testing and Photovoltaic Performance

An ideal nanostructured electrode should combine a large surface area with high adsorption of chromophores such as N719 and N3 dyes and speediness in the electron transfer processes of the TiO₂ film. This is particularly important once the nanostructured photoelectrode employed in such

photovoltaic materials is light absorption since multiple electron-hole pair generation becomes relevant [20]. Thus speediness and efficiency of photoelectrons generation are also keywords to evaluate the TiO₂ completion. It is clear that the importance of nanostructured electrodes for enhancing the performance of DSSC is a direct

expression of factors that determine photovoltaic efficiency. Such factors do not only include maximum power generation but also the energy conversion rate at the different processes in the photovoltaic device [12, 31]. The extent to which the performance of DSSC has benefited from the development of nanostructured thin films by doping TiO₂ with different metal oxide, which is derived from a high density of photon absorption, which could equally gain from using the same type of electrodes [12, 31]. The modified DSSCs Performance of the undoped TiO₂ and ZnO/ZnS doped TiO₂ (2%, 4%, and 6% wt.) were investigated from current-voltage (I-V) testing under standard test conditions (25 °C, 1 sun, AM1.5G) (shown in Figure 5). I-V characteristics provide information on the performance of the DSSCs, and the results are illustrated in Table 1. The following equation can calculate the power conversion efficiency of DSSCs [6, 33]:

$$FF = \frac{(J_m \times V_m)}{(J_{sc} \times V_{oc})} \quad \dots(1)$$

$$PCE = \frac{(J_{sc} \times V_{oc} \times FF)}{P_{in}} \times 100 \quad \dots(2)$$

The key parameters obtained from the IV curve are the short-circuit maximum voltage (V_m), the maximum current density (J_m), the short circuit current (J_{sc}), the open circuit voltage (V_{oc}), the fill factor (FF), the incident light (P_{in}), and finally, the power conversion efficiency (PEC) of the solar cell. The J_{sc} of fabricated DSSC are directly affected by the amount of ZnO/ZnS dopant in TiO₂. When the amount of doping increased, initially, the J_{sc} was increased from (8.74 mA/cm²) for undoped TiO₂ to (9.60 mA/cm²) for ZnO/ZnS 6%. According to the results of J_{sc}, The ZnO/ZnS 6% photoanode has a high electron diffusion coefficient and good electron injection between the dye and the surface of the photoanode. The surface properties and size of nanoparticles of the modified photoanode could be affected by the variation of J_{sc}. The best efficiency (4.92%) was presented in ZnO/ZnS 6% doped TiO₂, and that improvement of around 20% in solar cell devices compared to un-doped photoanode.

Table 1. The I-V curve characteristic of the three prepared nanocomposite

Types of photoanode	J _{sc} (mA/cm ²)	V _{oc} (V)	FF (%)	PCE (%)
Undoped TiO ₂	8.74	0.63	62.58	3.71
ZnO/ZnS (2% wt) doped TiO ₂	8.77	0.69	62.68	3.93
ZnO/ZnS (4% wt) doped TiO ₂	9.18	0.72	66.13	4.34
ZnO/ZnS (6% wt) doped TiO ₂	9.60	0.81	66.91	4.92

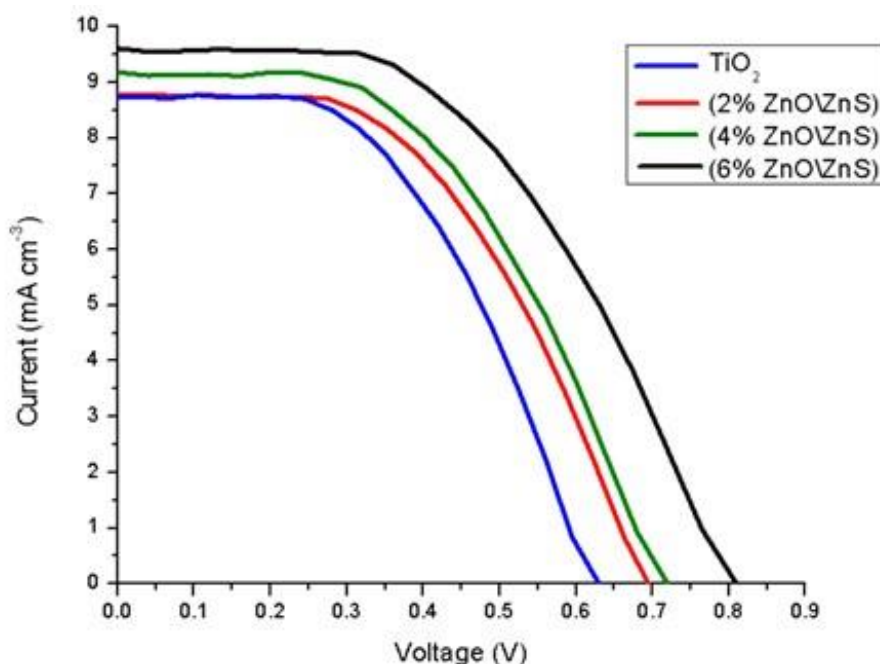


Figure 5. I-V curve of TiO₂, ZnO/ZnS (2%), ZnO/ZnS (4%), ZnO/ZnS (6%)

3. Conclusions

The ethanolic mixing method achieved the synthesis of a ZnO/ZnS nanocomposite, followed by characterization by SEM, XRD, and EDX. The SEM displays the two compounds at different magnification levels, revealing a high degree of mixing between them. The XRD of ZnO/ZnS analysis reveals that the ZnO/ZnS mixture exhibits a hexagonal wurtzite phase for ZnO and a cubic phase for ZnS. The ZnO/ZnS nanocomposite, which had been synthesized, was used as a dopant in various proportions (2%, 4%, and 6%) with TiO₂. Subsequently, it was employed as a photoanode in DSSCs. The results showed that adding 6% weight of ZnO/ZnS doped TiO₂ enhanced photovoltaic performance, reaching 4.92%. which has a high J_{sc} of 9.60 mA/cm² and Voc of 0.81 V suggests the presence of a high electron diffusion coefficient and effective electron injection between the dye and the surface of the photoanode.

Conflict of interest

There are no conflicts of interest.

Acknowledgment

The researchers acknowledged Al-Karkh University of Science and College of Education for Pure Science Ibn Al-Haitham for support and funding.

Funding: No funds have been received for this research

References

- [1] Abdallah, M.; Hussain, Z.; Thamer, H. ; Abd Ali, A.; Yousif, E.; Mohammed, S.; "Nanomaterials and Energy Storage in a Glance: a Review". Al-Nahrain J. Sci. 24(2): 21-26, 2021.
- [2] Abdalhadi, S.; Mohammed, N.; Ali, K.; Al-zubaidi, H.; "Investigating the Effects of Fluorine Substituents on Organic Dyes in Dye-Sensitized Solar Cells". J. Turk. Chem. Soc., Sect. A, 11(1): 1-10, 2024.
- [3] Mohammed, M. K. A.; Abdalhadi, S. M.; Kumar, A.; Doshi, O. P.; Al-Mousoi, A. K.; Hussein, H. T.; et al.; "Designing a Novel Hole-Transporting Layer for FAPbI₃-Based Perovskite Solar Cells". Energy Fuels, 37(24): 19870-19881, 2023.
- [4] Mohammed, N.; Shakkor, S. J.; Abdalhadi, S. M.; Al-Bayati, Y. K.; "Two multifunctional benzoquinone derivatives as small molecule organic semiconductors for bulk heterojunction and perovskite solar cells". Main Group Chem., 21: 943-952, 2022.
- [5] Cariello, M.; Abdalhadi, S. M.; Yadav, P.; Decoppet, J.-D.; Zakeeruddin, S. M.; Grätzel, M.; et al.; "An investigation of the roles furan versus thiophene π -bridges play in donor- π -acceptor porphyrin based DSSCs". Dalton Trans., 47(18): 6549-6556, 2018.
- [6] Abdalhadi, S. M.; Al-Baitai, A. Y.; Al-Zubaidi, H.; "Synthesis and characterization of 2, 3-diaminomaleonitrile derivatives by one-pot schiff base reaction and their application in dye synthesized Solar cells". Indones. J. Chem., 21(2): 443-451, 2020.
- [7] Sarmad S. Al-Obaidi, Ali A. Y.; "Synthesis Of Nanostructured TiO₂ Thin Films By Pulsed Laser Deposition (PLD) And The Effect Of Annealing Temperature On Structural And Morphological Properties" Ibn al-Haitham j. pure appl. sci. 26 (3), 143-152, 2013.
- [8] Dhanasekaran, P. and R. Marimuthu, A.; "Review on Dye-Sensitized Solar Cells (DSSCs), Materials and Applications". Int. J. Eng. Sci., 20(1): 1-23, 2023.
- [9] Hamadalla, H.D. and Ali F.H.; "Study of the Optical and Structural Properties of Metal-Doped Titanium Dioxide Electrode Prepared by the Sol-Gel Method for Dye-Sensitized Solar Cells". Iraqi J. Phys., 22(2): 57-68, 2024.
- [10] Belessiotis, G. V.; Antoniadou, M.; Ibrahim, I.; Karagianni, C. S.; Falaras, P.; "Universal electrolyte for DSSC operation under both simulated solar and indoor fluorescent lighting". Mater. Chem. Phys., 277: 125543, 2022.
- [11] Kareem, A.A., Jaffer H.I., and Al-Lamy H.K.; "Photoconductivity of An Inorganic /Organic Composites Containing Dye-Sensitized (Zinc Oxide)". Ibn al-Haitham j. pure appl. sci, 26(1): 123-130, 2017.
- [12] Kokkonen, M.; Talebi, P.; Zhou, J.; Asgari, S.; Soomro, S. A.; Elsehrawy, F.; et al.; "Advanced research trends in dye-sensitized solar cells". J. Mater. Chem., 9(17): 10527-10545, 2021.
- [13] Safa K. M., Raied K. J., Kadhim A. A.; "Studying the Effect of Annealing on Optical and Structure Properties of ZnO Nanostructure Prepared by Laser Induced Plasma." Iraqi J. Sci., 60(10), 2168-2176, 2019
- [14] Satpute, S. D.; Bhujbal, P. K.; Shaikh, S. F.; Patil, S. A.; Jadkar, S. R.; More, S. A.; "TiO₂ blocking layer incorporated TiO₂/In₂O₃-based photoanode for DSSC application". J. Mater. Sci.: Mater. Electron. 34(36): 2311, 2023.
- [15] Singh, A.; Saini, Y. K.; Kumar, A.; Gautam, S.; Kumar, D.; Dutta, V. et al.; "Property Modulation of Graphene Oxide Incorporated

- with TiO₂ for Dye-Sensitized Solar Cells". ACS omega, 7(48): 44170-44179, 2022.
- [16] Saravanan, S. and Dubey R.S.; "Optical and morphological studies of TiO₂ nanoparticles prepared by sol-gel method". Mater. Today, 47: 1811-1814, 2021.
- [17] Rahma, A.J., Oleiwi H.F., and Abbas H.A.; "Synthesis of TiO₂ Nanoparticles Using Spin-Coating and Drop-Casting Techniques for Antibacterial Application.", J. Nanostruct, 13(3), 673-684, 2023.
- [18] Sekar, R.; Sivasamy, R.; Ricardo, B.; Manidurai, P. J.; "Ultrasonically synthesized TiO₂/ZnS nanocomposites to improve the efficiency of dye sensitized solar cells". Mater. Sci. Semicond. Process., 132: 105917, 2021.
- [19] Amjed A. M., Mouruj A. A.; "Assessment the Modulation effect of using Green synthesis ZnO NPs against Multidrug Resistant Klebsiella pneumoniae isolated from respiratory tract infection." Iraqi J. Sci, 60(6), 1221-1231, 2019.
- [20] Niu, H.; Yao, X.; Luo, S.; Xie, Y.; Li, T.; Chen, W.; et al.; "Combination of multiple routes to enhance DSSC performance: Flower-like structure of SnO₂ as photoanode and modification with Ag nanoparticle". Mater. Sci. Semicond. Process., 177: 108363, 2024.
- [21] Tuama M. J. and Alias M. F.; "Synthesis of ZnO:ZrO₂ Nanocomposites Using Green Method for Medical Applications." KIJOMS, 10(3), 418-430, 2024.
- [22] Rao, S. S.; Punnoose, D.; Tulasivarma, C. V.; Kumar, C. P.; Gopi, C. V.; Kim S.; et al.; "A strategy to enhance the efficiency of dye-sensitized solar cells by the highly efficient TiO₂/ZnS photoanode". Dalton Trans., 44(5): 2447-2455, 2015.
- [23] Sharma, M.; Gupta, S.; Prasad, S.; Bharatiya, P. K.; Mishra, D. J.; "First principles study of the influence of metallic-doping on crystalline ZnS: From efficiency aspects for use in a ZnS based dye sensitized solar cell (DSSC)". Photonic and Acousto Optic., 194(1): 96-103, 2018.
- [24] Afrooz, M.; Dehghani, H.; Khalili, S. S.; Firoozi, N. J.; "Effects of cobalt ion doped in the ZnS passivation layer on the TiO₂ photoanode in dye sensitized solar cells based on different counter electrodes". Synth. Met., 226: 164-170, 2017.
- [25] Nurazizah, E. S.; Fajariah, A. R.; Aprilia, A.; Safriani, L. J.; "Performance Improvement of Dye-Sensitized Solar Cells Using a Combination of TiO₂ and ZnO as Photoanodes". J. Mater. Eng, 950: 25-30, 2023.
- [26] Jamal, R.K., Hameed M.A., and Adem K.A.; "Optical properties of nanostructured ZnO prepared by a pulsed laser deposition technique." Mater. Lett., 132, 31-33. 2014.
- [27] Eom, T. S.; Kim, K. H.; Bark, C. W.; Choi, H. W. J.; Crystals, L.; "Influence of Fe₂O₃ doping on TiO₂ electrode for enhancement photovoltaic efficiency of dye-sensitized solar cells". J. Opt., 600(1): 39-46, 2014.
- [28] Alinezhad, H.; Tajbakhsh, M.; Salehian, F.; Biparva, P. J.; "Synthesis of quinoxaline derivatives using TiO₂ nanoparticles as an efficient and recyclable catalyst". Bull. Korean Chem. Soc., 32(10): 3720-3725, 2011.
- [29] Jayabal, P.; Gayathri, S.; Sasirekha, V.; Mayandi, J.; Ramakrishnan, V.; "Preparation and characterization of ZnO/graphene nanocomposite for improved photovoltaic performance." J. Nanoparticle Res., 16(11): 2640, 2014.
- [30] Buraihi, A., Abdalameer, N., Farman Ahialy, N., Mutter, M.; "Synthesis and Characterization of ZnS:Cu Thin Films as Gas Sensor Application", IREA, 12 (2), 94-102, 2024.
- [31] Ako, R. T.; Ekanayake, P.; Young, D. J.; Hogley, J.; Chellappan, V.; Tan, A. L.; et al., "Evaluation of surface energy state distribution and bulk defect concentration in DSSC photoanodes based on Sn, Fe, and Cu doped TiO₂". Appl. Surf. Sci., 351: 950-961, 2015.
- [32] Ramadhani, D. A. K.; Sholeha, N.; Khusna, N. N.; Diantoro, M.; Afandi, A. N.; Osman, Z.; et al., "Ag-doped TiO₂ as photoanode for high performance dye sensitized solar cells". Mater. Sci. Energy Technol., 7: 274-281, 2024.
- [33] Abdulhussein, S.F., Abdalhadi S.M., and Hanoon H.D.; "Synthesis of new imidazole derivatives dyes and application in dye sensitized solar cells supported by DFT." Egypt. J. Chem., 65(9): 211-217, 2022.